

AperTO - Archivio Istituzionale Open Access dell'Università di Torino

**Ultrahigh-pressure metamorphism and multistage exhumation of eclogite of the Luotian dome, North Dabie Complex Zone (central China): Evidence from mineral inclusions and decompression textures.**

**This is the author's manuscript**

*Original Citation:*

*Availability:*

This version is available <http://hdl.handle.net/2318/127404> since

*Published version:*

DOI:10.1016/j.jseaes.2010.10.016

*Terms of use:*

Open Access

Anyone can freely access the full text of works made available as "Open Access". Works made available under a Creative Commons license can be used according to the terms and conditions of said license. Use of all other works requires consent of the right holder (author or publisher) if not exempted from copyright protection by the applicable law.

(Article begins on next page)



## UNIVERSITÀ DEGLI STUDI DI TORINO

This Accepted Author Manuscript (AAM) is copyrighted and published by Elsevier. It is posted here by agreement between Elsevier and the University of Turin. Changes resulting from the publishing process - such as editing, corrections, structural formatting, and other quality control mechanisms - may not be reflected in this version of the text. The definitive version of the text was subsequently published in:

*Journal of Asian Earth Sciences* (2011), 42, 4: p. 607–17, doi:10.1016/j.jseaes.2010.10.016.

You may download, copy and otherwise use the AAM for non-commercial purposes provided that your license is limited by the following restrictions:

- (1) You may use this AAM for non-commercial purposes only under the terms of the CC-BY-NC-ND license.
- (2) The integrity of the work and identification of the author, copyright owner, and publisher must be preserved in any copy.
- (3) You must attribute this AAM in the following format: Creative Commons BY-NC-ND license (<http://creativecommons.org/licenses/by-nc-nd/4.0/deed.en>), [+ *Digital Object Identifier link to the published journal article on Elsevier's ScienceDirect® platform*]

Manuscript Number: JAES-D-10-00055

Title: Ultrahigh-pressure metamorphism and multistage exhumation of eclogite from the Luotian dome, North Dabie Complex Zone (central China): Evidence from mineral inclusions and decompression texture

Article Type: SI: HP-UHP metamorphic rocks

Keywords: Eclogite; Coesite; Ultrahigh-pressure metamorphism; Multistage exhumation; North Dabie Complex Zone

Corresponding Author: Professor Yican Liu, Ph.D.

Corresponding Author's Institution:

First Author: Yican Liu, Ph.D.

Order of Authors: Yican Liu, Ph.D.; Xiaofeng Gu; Franco Rolfo; Zhenyu Chen

Abstract: The studied eclogite is located in the Luotian dome in the southwestern part of the North Dabie Complex Zone (NDZ), central China, and is a portion of deeply subducted mafic lower continental crust of the South China Block. Petrologic analysis suggests that the eclogite underwent ultrahigh-pressure (UHP) and high-pressure eclogite-facies metamorphism, and subsequent HP granulite-facies overprinting and amphibolite-facies retrogression during continental subduction and exhumation. As a result, multiple decompression textures were produced, suggesting a multistage exhumation history from eclogite-, to granulite-, to amphibolite-facies conditions. A striking feature of this eclogite is the widespread exsolution of different phases: oriented needles of rutile + clinopyroxene + amphibole + apatite in garnet; quartz + amphibole + hyperthene + sodic plagioclase in clinopyroxene; pyrrhotite in apatite. Most importantly, we provide for the first time conclusive evidence of quartz pseudomorphs after coesite in garnet and relic coesite (confirmed by in situ Raman spectroscopy) in zircon. In addition, there are two groups of apatite: one is fluor (F)-apatite and occurs as inclusion in garnet or in matrix, which is rich in F (23 wt %) without any exsolutions and formed at UHP metamorphic conditions; the second is relatively poor in F (< 1 wt %) associated with the oriented pyrrhotite exsolution and formed during decompression. Microtextural and petrologic analysis suggest that the eclogites from southwestern segment of the NDZ are similar to eclogites from the northern segment of the NDZ (e.g., Huangweihe and Baizhangyan) and suffered UHP metamorphism with pressure peak  $\geq$  5-7 GPa. These results, combined with published geochronological data, imply that the NDZ wholly experienced Triassic UHP metamorphism as a coherent unit.

1        **Ultrahigh-pressure metamorphism and multistage exhumation of**  
2        **eclogite from the Luotian dome, North Dabie Complex Zone (central**  
3        **China): Evidence from mineral inclusions and decompression texture**

4

5                    Yi-Can Liu <sup>a,\*</sup>, Xiao-Feng Gu <sup>a</sup>, F. Rolfo <sup>b</sup> and Zhen-Yu Chen <sup>c</sup>

6

7        a. CAS Key Laboratory of Crust-Mantle Materials and Environments, School of Earth and Space

8                    Sciences, University of Science and Technology of China, Hefei 230026, China

9        b. Department of Mineralogical and Petrological Sciences, University of Torino, Via Valperga

10                   Caluso 35, 1-10125 Torino, Italy

11        c. Institute of Mineral Resources, Chinese Academy of Geological Sciences, Beijing 100037,

12                    China

13

14

15

16

17

18

19        \*Corresponding author. Tel.: +86 551 3600367.

20        *E-mail address:* [liuyc@ustc.edu.cn](mailto:liuyc@ustc.edu.cn) (Yi-Can Liu)

21

## ABSTRACT

22  
23 The studied eclogite is located in the Luotian dome in the southwestern part of the  
24 North Dabie Complex Zone (NDZ), central China, and is a portion of deeply  
25 subducted mafic lower continental crust of the South China Block. Petrologic analysis  
26 suggests that the eclogite underwent ultrahigh-pressure (UHP) and high-pressure  
27 eclogite-facies metamorphism, and subsequent HP granulite-facies overprinting and  
28 amphibolite-facies retrogression during continental subduction and exhumation. As a  
29 result, multiple decompression textures were produced, suggesting a multistage  
30 exhumation history from eclogite-, to granulite-, to amphibolite-facies conditions. A  
31 striking feature of this eclogite is the widespread exsolution of different phases:  
32 oriented needles of rutile + clinopyroxene + amphibole + apatite in garnet; quartz +  
33 amphibole + hyperthene + sodic plagioclase in clinopyroxene; pyrrhotite in apatite.  
34 Most importantly, we provide for the first time conclusive evidence of quartz  
35 pseudomorphs after coesite in garnet and relic coesite (confirmed by in situ Raman  
36 spectroscopy) in zircon. In addition, there are two groups of apatite: one is fluor  
37 (F)-apatite and occurs as inclusion in garnet or in matrix, which is rich in F (~3 wt %)  
38 without any exsolutions and formed at UHP metamorphic conditions; the second is  
39 relatively poor in F (< 1 wt %) associated with the oriented pyrrhotite exsolution and  
40 formed during decompression. Microtextural and petrologic analysis suggest that the  
41 eclogites from southwestern segment of the NDZ are similar to eclogites from the  
42 northern segment of the NDZ (e.g., Huangweihe and Baizhangyan) and suffered UHP  
43 metamorphism with pressure peak > 5-7 GPa. These results, combined with published

44 geochronological data, imply that the NDZ wholly experienced Triassic UHP  
45 metamorphism as a coherent unit.

46

47 **Key words:** Eclogite; Coesite; Ultrahigh-pressure metamorphism; Multistage  
48 exhumation; North Dabie Complex Zone

## 49 **1. Introduction**

50       The oriented exsolution or lamellae is a common feature of minerals that derive  
51 from deep-seated sources such as kimberlites, diamondiferous rocks, as well as  
52 eclogites and related rocks from high-pressure (HP) to ultrahigh-pressure (UHP)  
53 metamorphic belts, and is interpreted as the result of cooling and decompression (e.g.,  
54 Smith, 1984; Gayk et al., 1995; Zhang et al., 1995, 2002a, 2005; Katayama et al.,  
55 2000a; Tsai and Liou, 2000; Ye et al., 2000a; Dobrzhinetskaya et al. 2002; Song et al.,  
56 2003, 2005; Malaspina et al., 2006; Nakano et al., 2007 and references therein). This  
57 peculiar microtexture is generally used to infer the primary conditions under which  
58 eclogites and related metamorphic rocks were formed. Eclogites are considered to be  
59 the most important witnesses of continental subduction, collision and subsequent  
60 exhumation processes and thus provide important information on the geodynamics of  
61 orogens. The survival of coesite and other index minerals in UHP rocks has important  
62 implications for the exhumation of subducted crustal rocks and is most commonly  
63 attributed to rapid exhumation, continuous cooling during uplift, and inclusion in  
64 strong phases that can sustain a high internal over-pressure during decompression  
65 (Mosenfelder et al., 2005). However, peak metamorphic conditions and the  
66 pressure/temperature (PT) evolution of UHP rocks involved in multistage  
67 metamorphism are not always straightforward because their mineral assemblages have  
68 been re-equilibrated to various degrees during retrogression and decompression (e.g.,  
69 Faryad, 2009).

70       The finding of coesite and micro-diamond in eclogites from the Dabie orogen in

71 central China (Okay et al., 1989; Wang et al., 1989; Xu et al., 1992) led this area to be  
72 one of the most important targets for studying UHP metamorphism, documenting  
73 continental subduction to mantle depths. A great number of studies have contributed  
74 to the understanding of the geodynamics of subduction and exhumation resulting in  
75 the Dabie–Sulu orogenic belt (see Liu and Li, 2008 for a summary). This orogenic  
76 belt contains the largest exposure of UHP rocks in the world, which formed by  
77 Triassic continental collision between the South China and North China Blocks (e.g.,  
78 Li et al., 1993, 2000; Chavagnac and Jahn, 1996; Hacker et al., 1998; Ayers et al.,  
79 2002; Liu et al., 2005, 2007a, 2007b).

80 The Dabie UHP metamorphic belt in central China consists of three  
81 eclogite-bearing UHP crustal slices from north to south: the North Dabie complex  
82 zone (NDZ), the Central Dabie UHP metamorphic zone (CDZ), and the South Dabie  
83 low-T eclogite zone (SDZ), which differ by rock association, protolith nature and  
84 metamorphic evolution (see Liu and Li, 2008, in detail). Moreover, Pb isotopic  
85 mapping on the Dabie UHP belt has revealed a clear detachment between deeply  
86 subducted upper continental crust (the CDZ) and felsic lower crust (the NDZ) (Zhang  
87 et al., 2002a; Li et al., 2003). This duality is also supported by their different  
88 termination ages of peak UHP metamorphism, which probably result from multistage  
89 detachment within deeply subducted crust at different depths and multi-slice  
90 successive exhumation of the UHP rocks during continental collision (Liu et al.,  
91 2007b; Liu and Li, 2008). However, because of the lack of critical UHP phases such  
92 as coesite or microdiamond in the southwestern part of the NDZ, whether or not the



93 NDZ as a whole underwent deep subduction and subsequent UHP metamorphism is  
94 still a controversial issue (Zhao et al., 2008; Zhang et al., 2009).

95 In order to clarify : (1) peak metamorphic conditions of the eclogite from the  
96 Luotian dome in the southwestern part of the NDZ; (2) if the NDZ wholly underwent  
97 UHP metamorphism, a petrologic study on the eclogite from the Luotian dome in the  
98 NDZ was carried out. This paper focuses on multiple decompression texture and UHP  
99 metamorphic evidence of these eclogites. The results not only provide direct evidence  
100 on UHP metamorphism and multistage breakdown processes on the eclogite in the  
101 area, but also provide new constraints on exhumation mechanism of the UHP rocks in  
102 the Dabie orogen.

103

## 104 **2. Geologic background and sample**

105 The Dabie orogen is located in the intermediate segment of the  
106 Qinling-Dabie-Sulu belt formed by the collision of the North China Block and South  
107 China Block (SCB) in the Triassic. It comprises several fault-bounded rock units with  
108 varying metamorphic grades and is generally subdivided into five major lithotectonic  
109 units from north to south (e.g., Okay et al., 1993; Xu et al., 2003, 2005; Li et al., 2004;  
110 Liu et al., 2005, 2007a, 2007b; Liu and Li, 2008): (1) the Beihuaiyang zone (BZ); (2)  
111 the North Dabie complex zone (NDZ); (3) the Central Dabie UHP metamorphic zone  
112 (CDZ); (4) the South Dabie low-T eclogite zone (SDZ); and (5) the Susong complex  
113 zone (SZ). These five zones are respectively separated by the Xiaotian-Mozitan fault  
114 (XMF), Wuhe-Shuihou fault (WSF), Hualiangting-Mituo fault (HMF) and

115 Taihu-Shanlong fault (TSF) (Fig. 1). Zone (1) is a low-grade composite unit  
116 comprising the Foziling (or Xinyang) Group and the Luzhenguan (or Guishan)  
117 complex, whereas Zones (2), (3), (4) and (5) belong to the subducted SCB.

118 UHP metamorphic rocks, including coesite-bearing eclogite, UHP gneiss,  
119 whiteschist, quartz jadeitite and marble with eclogite nodules, are observed in the  
120 CDZ and SDZ (e.g., Xu et al., 1992; Okay, 1993; Okay et al., 1993; Rolfo et al., 2000;  
121 Li et al., 2004). The occurrence of diamond and coesite in the UHP rocks from the  
122 CDZ indicates the UHP metamorphism occurred at 700–850 °C and >2.8 GPa (e.g.,  
123 Okay et al., 1989; Wang et al., 1989; Xu et al., 1992; Okay, 1993; Rolfo et al., 2004),  
124 whereas the peak P-T conditions on the eclogites in the SDZ were estimated at 670 °C  
125 and 3.3 GPa (Li et al., 2004). Both the CDZ and SDZ units experienced UHP  
126 eclogite-facies, and subsequent HP eclogite- and amphibolite-facies retrograde  
127 metamorphism (e.g., Xu et al., 1992; Okay, 1993; Rolfo et al., 2004; Li et al., 2004).

128 The NDZ consists predominantly of banded tonalitic and granitic gneiss and  
129 post-collisional intrusions with subordinated meta-peridotite (including dunite,  
130 harzburgite and lherzolite), garnet pyroxenite, garnet-bearing amphibolite, granulite  
131 and eclogite. Although no coesite has not yet been discovered from the eclogite or  
132 gneiss in the NDZ, the occurrence of micro-diamond from eclogite and gneiss is a key  
133 evidence for UHP metamorphism (Xu et al., 2003, 2005; Liu et al., 2007b). In  
134 addition, quartz rods in clinopyroxene are widespread in the eclogite, and these  
135 exsolutions are commonly regarded as evidence of prior UHP metamorphism (e.g.,  
136 Smith, 1984; Liou et al., 1998; Tsai and Liou, 2000; Liu et al., 2005, 2007a; Zhang et

137 al., 2005). Therefore, also the eclogites from the NDZ underwent the UHP  
138 metamorphism at  $P > 3.5\text{--}4.0$  GPa (Xu et al., 2003, 2005; Malaspina et al., 2006). As  
139 concerning geochronology, Triassic zircon U-Pb (Liu et al., 2000) and Sm-Nd (Liu et  
140 al., 2005) ages of the eclogites from the NDZ suggest that they formed by subduction  
141 of the SCB in the Triassic, similar petrogenesis to those from the CDZ and SDZ. The  
142 Triassic metamorphic ages (Liu et al., 2000, 2007b; Bryant et al., 2004; Xie et al.,  
143 2004) and the occurrence of micro-diamonds in zircons (Liu et al., 2007b) from the  
144 banded gneisses in the NDZ suggest that also the gneisses surrounding the eclogites  
145 were involved in the continental deep subduction of the SCB. Following the UHP and  
146 HP eclogite-facies metamorphism, however, the eclogites from the NDZ were first  
147 subjected to granulite-facies overprinting, and later to amphibolite-facies retrogression  
148 (e.g., Liu et al., 2000, 2005; Xu et al., 2000). This peculiar P-T path suggests a  
149 different post-peak metamorphic evolution for different tectonic units (e.g., NDZ and  
150 CDZ) of the Dabie UHP belt. Therefore, although both the CDZ and NDZ units  
151 experienced UHP metamorphism, they had different exhumation histories, suggesting  
152 that CDZ and NDZ are two UHP slices decoupled after subduction (Xu et al., 2005;  
153 Liu et al., 2005, 2007a, 2007b; Liu and Li, 2008). As concerning the metamorphic  
154 history prior to the peak, Pb isotope investigations show that the UHP rocks from the  
155 CDZ are characterized by high radiogenic Pb while banded gneiss from the NDZ are  
156 characterized by low radiogenic Pb (Zhang et al., 2002a; Li et al., 2003); this suggests  
157 that the UHP rocks of the CDZ were derived from subducted upper crust, while the  
158 UHP rocks of the NDZ were derived from subducted felsic lower continental crust

159 with minor mafic boudins or lenses (Li et al., 2003; Liu et al., 2007a, 2007b).

160 A peculiar geologic feature in the southwestern segment of the NDZ is the  
161 Luotian dome, which is a deeply eroded area with abundant felsic and mafic  
162 granulites around the Luotian county (Fig. 1). In the Luotian dome, unusual eclogites  
163 were found as lenses in garnet-bearing banded tonalitic gneisses (Liu et al., 2007a).  
164 These eclogites preserve early granulite-facies mineral relics and have been  
165 overprinted by regionally extensive HP granulite-facies metamorphism, followed by  
166 penetrative amphibolite-facies retrogression during exhumation. The eclogite-facies  
167 mineral assemblage is garnet and relict omphacite, with rutile, quartz, allanite and  
168 fluor-apatite as common constituents. While micro-diamonds were found in the  
169 northeastern part of the NDZ, no index UHP minerals such as coesite and  
170 micro-diamond were identified so far in southwestern part of the NDZ, i.e. in the  
171 Luotian dome area. Because of the lack of index UHP phases, it has been always  
172 difficult to determine accurately the peak conditions under which the eclogites were  
173 formed, thus feeding a number of arguments on the tectonic affinity and evolution of  
174 the NDZ.

175 The eclogites from the Luotian dome occur as bands, lenses and blocks, up to 3m  
176 thick (Fig. 2), and are often strongly retrogressed to (garnet) amphibolite. The studied  
177 samples were collected from Luotian (sample 03LT1-1), Jinjiapu (samples 03LT8-1,  
178 06LT3-2 and 06LT4-2) and Shiqiaopu (samples 07LT6-1 and 09LT2-1), respectively  
179 (Fig. 1). Details of the petrography and mineral chemistry of the studied samples were  
180 given in a separate paper (Liu et al., 2007a) and are only summarized here. However,

181 samples were chosen because of their relative abundance of mineral inclusions in  
182 zircon and garnet, and oriented mineral exsolutions in garnet, clinopyroxene and  
183 apatite. Sample 03LT1-1 is a strongly retrogressed eclogite, which is mainly  
184 composed of garnet, rutile, hornblende and plagioclase with minor quartz, diopside,  
185 hypersthene and ilmenite. Other eclogite samples are less retrogressed and are  
186 composed of garnet, omphacite, diopside and rutile, and minor hypersthene,  
187 hornblende, plagioclase, quartz and ilmenite. Despite the strongly pervasive granulite-  
188 and amphibolite-facies overprint, five metamorphic stages have been recognized for  
189 the eclogite of the NDZ (Liu et al., 2005, 2007a, 2010): (1) a granulite-facies stage,  
190 with  $P \sim 0.8$  GPa; (2) a UHP eclogite-facies stage, with  $P = 4.0$  GPa and  $T = 900\text{--}960$   
191  $^{\circ}\text{C}$ , witnessed by the occurrence of diamond (Xu et al., 2003, 2005; Liu et al., 2007b)  
192 and oriented mineral exsolutions in garnet and clinopyroxene (Tsai et al., 2000; Xu et  
193 al., 2003, 2005; Liu et al., 2007a; Malaspina et al., 2006); (3) a HP eclogite-facies  
194 stage, with  $P = 2.0$  GPa and  $T = 800\text{--}900$   $^{\circ}\text{C}$ , characterized by the coexistence of  
195 garnet, sodic clinopyroxene or jadeite-poor omphacite and rutile with quartz; (3) a  
196 retrograde granulite-facies stage, with  $P = 1.1\text{--}1.4$  GPa and  $T = 804\text{--}857$   $^{\circ}\text{C}$ , indicated  
197 by the presence of hypersthene, plagioclase and diopside symplectite; (4) a retrograde  
198 amphibolite-facies stage, with  $P = 0.6\text{--}0.7$  GPa and  $T = 706\text{--}777$   $^{\circ}\text{C}$ .

199

### 200 **3. Analytical methods**

201 Mineral inclusions in zircon and oriented needles in garnet and clinopyroxene  
202 were identified using Raman spectroscopy at the Continental Dynamics Laboratory,

203 Chinese Academy of Geological Sciences (CAGS) and confirmed using the electron  
204 microprobe analyzer (EMPA) at the Institute of Mineral Resources, CAGS in Beijing.  
205 Furthermore, minerals relevant for this study were analyzed with a JEOL JXA-8800R  
206 EMPA at the Institute of Mineral Resources, CAGS in Beijing, The analytical  
207 conditions on the Raman and EMPA were reported by Xu et al. (2005) and Liu et al.  
208 (2009). The representative mineral compositions are presented in Table 1. The  
209 representative Raman spectra of mineral inclusions in zircon are reported in Fig. 6.  
210 Mineral abbreviations in figures and tables are after Kretz (1983).

211

## 212 **4. Decompression textures**

### 213 *4.1. Double symplectites*

214 In the studied samples, garnets are characterized by peculiar kelyphytic rims with  
215 two distinct reaction stages here referred as “double symplectites” (Fig. 3a and b): the  
216 fine-grained inner one is composed of amphibole and plagioclase and is inferred to  
217 derive from the decomposition of garnet during the amphibolite-facies retrogression;  
218 the outer symplectite between garnet and clinopyroxene or omphacite is mainly  
219 composed of very fine-grained hypersthene, diopside and plagioclase, and formed  
220 between reacting garnet and clinopyroxene under granulite-facies conditions; this  
221 outer symplectite is restricted to a very narrow zone. Both symplectites show  
222 vermicular texture and are devoid of mica, suggesting that the retrogressive reaction  
223 or decompression breakdown developed under fast exhumation rates and anhydrous  
224 conditions, such that the neoblastic minerals had insufficient time for recrystallization

225 and occurred as symplectite, *i.e.* a rapid retrograde metamorphic process from  
226 eclogite- via granulite- and amphibolite-facies conditions (Liu et al., 2005, 2007a).

227

#### 228 4.2. Needle exsolutions

229 A most spectacular feature of the eclogite in the NDZ is the ubiquitous  
230 occurrence of oriented needle exsolutions of different phases in clinopyroxene, garnet  
231 and apatite (Figs. 4a-d and 5a).

232 Oriented rods or needles in clinopyroxene can be divided into three types  
233 depending on their mineral assemblage. Type 1 clinopyroxene contains quartz rods  
234 (Fig. 4a), which have been considered to be the evidence for the prior existence of a  
235 supersilicic omphacite stable at UHP conditions ( $\geq 2.5$  GPa) (cf. Liou et al., 1998 for  
236 a review), and occur as discrete grains in the matrix or as inclusions in garnet. Type 2  
237 clinopyroxene contains quartz + sodic plagioclase + orthopyroxene + amphibole  
238 needles (Fig. 4b). Type 3 clinopyroxene contains quartz + orthopyroxene lamellae  
239 (Fig. 4c). All these microtextures show that the precursor clinopyroxene was rich in Si  
240 and Na during the peak metamorphic conditions. Worth of note is that  
241 ultrahigh-temperature (UHT) conditions ( $> 900$  °C; Harley, 1998) may be suggested  
242 by orthopyroxene lamellae from clinopyroxene (type 3) as reported by Nakano et al.  
243 (2007). However, although UHT metamorphic conditions of 905–917 °C can be  
244 inferred by applying Cpx-Opx geothermometry (Wood and Banno, 1973; Wells, 1977)  
245 to the hypersthene lamellae and the host clinopyroxene at their contact, more data are  
246 needed to better constrain this event and to define its geological significance.

247 Most of oriented rods or needles in garnet are rutile; few garnet crystals host  
248 rutile + clinopyroxene + amphibole + apatite needles (Fig. 4d), which attest to the  
249 presence of a Si-Ti-Na-P-rich precursor garnet phase (majorite) stabilized at UHP  
250 conditions (> 5–7 GPa) (Ye et al., 2000a; Mposkos and Kostopoulos, 2001; Song et  
251 al., 2005).

252 Needle exsolutions in apatite are made of pyrrhotite. The studied samples contain  
253 two types of apatite: type 1 is fluor (F)-apatite and occurs as inclusion in garnet or in  
254 the matrix, and is rich in F (~3 wt %) and devoid of any exsolutions; type 2 apatite is  
255 relatively poor in F (< 1 wt %) and is typically associated with the oriented pyrrhotite  
256 exsolution (Figs. 3d and 5a; Table 1). Type 1 apatite make a stable assemblage with  
257 the peak minerals such as garnet, omphacite, rutile and coesite (see below) and hence  
258 formed at UHP metamorphic conditions. The UHP origin of type 1 apatite is also  
259 supported by its high F contents because it has been demonstrated that F in apatite  
260 increases with metamorphic grade and pressure (Spear and Pyle, 2002). In contrast,  
261 type 2 apatite may be the result of breakdown during decompression.

262

### 263 4.3. *Quartz inclusions*

264 Quartz inclusions in garnet from the studied eclogites always show sub-rounded  
265 to elliptical shapes and occur both as single crystals, and as polycrystalline aggregates  
266 50 to 150  $\mu\text{m}$  in size (Figs. 3c and 4f). Around single large monocrystalline and  
267 polycrystalline quartz inclusions (> 30  $\mu\text{m}$ ), tensional cracks are typically developed  
268 radiating into garnet (Fig. 3c), whereas only a few irregular joints are present around



269 very small ( $< 10 \mu\text{m}$ ) quartz inclusions. For other mineral inclusions, radial fracturing  
270 of garnet is much less common. The observed textural characters of the quartz  
271 inclusions are commonly indicated as decompression features and are often  
272 considered as diagnostic for the identification of quartz pseudomorphs after coesite  
273 within a rigid host (Chopin, 1984).

274

#### 275 *4.4. Coesite relics*

276 Zircon is probably the best container for relict UHP metamorphic phases because  
277 of its chemical inactivity and extreme stability over a wide P–T interval (e.g., Chopin  
278 and Sobolev, 1995; Liou et al., 1998; Tabata et al., 1998; Parkinson and Katayama,  
279 1999). It has been widely used to determine the presence of UHP phases, including  
280 coesite and diamond in country rock gneisses and to establish the P–T path of deeply  
281 subducted terranes (e.g., Tabata et al., 1998; Katayama et al., 2000b; Ye et al., 2000b;  
282 Liu et al., 2001, 2002, 2007b).

283 Recently Liu et al. (2010) analyzed by Raman spectroscopy, a number of quartz  
284 inclusions in zircon from one of the retrograded eclogite studied in this paper (sample  
285 03LT1-1) and found a strong peak of quartz at  $466 \text{ cm}^{-1}$  but also a weak peak of  
286 coesite at  $521 \text{ cm}^{-1}$  (Fig. 6). Such peaks represent fundamental vibrations of coesite  
287 along with the typical quartz vibration as reported from quartz-transformed coesite in  
288 UHP rocks (Ghiribelli et al., 2002; Liu et al., 2002; Zhang et al., 2005). This spectral  
289 feature strongly support the presence of trace relic coesite in quartz, which might have  
290 escaped its complete transformation during decompression.

291

## 292 **5. Discussion and interpretation**

### 293 *5.1. Coesite and other indicators of UHP metamorphism*

294 The discovery of coesite in crustal rocks (Chopin, 1984; Smith, 1984) first  
295 introduced a very powerful indicator of UHP metamorphism. Unlike diamonds, the  
296 presence of only one coesite inclusion undoubtedly provides evidence for an UHP  
297 origin of the host mineral (Korsakov et al., 2009). However, due to the reaction  
298 kinetics of the coesite to quartz transformation (Mosenfelder and Bohlen, 1997;  
299 Perrillat et al., 2003 and references therein), fresh coesite rarely survives even when it  
300 is included in robust minerals. In most cases, relics of coesite are present in the core  
301 of polycrystalline quartz aggregates, surrounded by a radial crack pattern (e.g.,  
302 Mosenfelder et al., 2005). These partial or complete pseudomorphs of quartz after  
303 coesite are ubiquitous over a wide range of lithologies in various orogens of different  
304 ages, and are typically involved in a multistage metamorphic history related to  
305 exhumation. These pseudomorphs are also typically used together with other  
306 mineralogical indicators to prove that the rocks experienced UHP metamorphic  
307 conditions.

308 In contrast to other sectors of the NDZ, micro-diamonds have not been found in  
309 the Luotian dome in the southwestern part of the NDZ; however, there are other clues  
310 supporting the UHP metamorphism over the whole unit.

311 Firstly, the occurrence of mineral quartz exsolutions. Although Page et al. (2005)  
312 suggested that the presence of quartz rods in clinopyroxene does not require UHP

313 metamorphism, relic coesite rods in eclogites of Tianshan in China (Zhang et al. 2005)  
314 clearly demonstrated that SiO<sub>2</sub> exsolution in clinopyroxene occurred in the coesite  
315 stability field and that most exsolved coesite rods in clinopyroxene transformed to  
316 quartz during retrograde metamorphism with only minor amounts of remnant coesite  
317 being present. Dobrzhinetskaya et al. (2002) proposed that oriented SiO<sub>2</sub> precipitation  
318 in omphacite from eclogite in the Alpe Arami garnet peridotite massif, Switzerland,  
319 occurred at P-T conditions of 7.0 GPa and 1100 °C. Experimental studies also  
320 indicated that supersilicic clinopyroxene formed under HP-UHP and HT conditions of  
321 2.5–3.2 GPa at 1400–1500 °C (Wood and Henderson 1978), 3.5–7.0 GPa at 1200 °C  
322 (Zharikov et al. 1984), and 2–3 GPa at 1200–1400 °C (Gasparik 1986). Mao (1971)  
323 found that at 4 GPa and 1100–1700 °C, clinopyroxene contains 7.5 wt% excess SiO<sub>2</sub>,  
324 and its excess SiO<sub>2</sub> increases with pressure. Therefore, based on natural and  
325 experimental data, quartz exsolution in clinopyroxene are fully compatible with, and  
326 strongly suggest, UHP and HT conditions because natural rocks containing  
327 clinopyroxene with quartz rods usually coexist with garnet or zircon containing  
328 coesite, or its quartz pseudomorph, or micro-diamond inclusions (e.g., Xu et al., 1992,  
329 2005; Zhang et al., 1995; Liou et al., 1998; Katayama et al. 2000; Liu et al., 2007b).  
330 In this regard, oriented rods or needles in clinopyroxene from the eclogites in the  
331 Luotian Dome most likely witness a former UHP stage as suggested by Tsai and Liou  
332 (2000), and this microtextural evidence is fully consistent with the presence of relic  
333 coesite in zircon from one of the studied samples. Additionally, garnet from the  
334 studied eclogites contains rutile + clinopyroxene + amphibole + apatite oriented

335 needles, which were ascribed by a number of authors (Ye et al., 2000a; Mposkos and  
336 Kostopoulos, 2001; Song et al., 2005) to be precursors of UHP condition at  $P > 5\text{--}7$   
337 GPa.

338 Another important evidence for UHP metamorphism in the studied area is the  
339 occurrence of quartz and relic coesite inclusions. Among all studied quartz inclusions  
340 in garnet, the majority is of the monocrystalline type (Fig. 3c), some are of the  
341 polycrystalline type (2 to 5 grains per inclusion, Fig. 4e and f), and only one inclusion  
342 within a zircon of sample 03LT1-1 gives Raman evidence of relic coesite based on the  
343 presence of an additional band at  $521\text{ cm}^{-1}$  in the spectrum (Fig. 6c), corresponding to  
344 the most intense fundamental vibration in coesite. Numerous studies on natural  
345 coesite samples have documented that fundamental coesite and quartz frequencies can  
346 be present in single coesite spectra (Boyer et al., 1985; Ghibelli et al., 2002; Liu et  
347 al., 2002; Zhang et al., 2005). This apparent discrepancy can be easily explained when  
348 the coesite grains are smaller than the laser beam to include some of the surrounding  
349 quartz, or because of incipient coesite transformation to quartz, although in some  
350 cases this effect can be induced by the laser itself. Moreover, a fracture goes through  
351 the coesite/quartz inclusions in zircon from sample 03LT1-1 (Fig. 6a), most likely  
352 resulting in the transformation of coesite to quartz.

353 In addition, a number of monocrystalline and polycrystalline quartz inclusions are  
354 enclosed in garnet with well-developed radial fractures (Figs. 3c and 4e), which are  
355 indicated as decompression features and are often considered to be diagnostic for the  
356 identification of quartz pseudomorphs after coesite within a rigid host (e.g., Chopin,

357 1984; Smith, 1984). However, although the presence of such textural features should  
358 be treated with caution because they are not unique to coesite transformation as  
359 suggested by Chopin & Sobolev (1995), the finding of relic coesite in the same rock  
360 samples supports the possibility that polycrystalline and monocrystalline quartz  
361 inclusions in garnet with radial cracks were formerly coesite, now inverted to quartz.

362 Therefore, the studied eclogites show radial fractures within garnet around quartz  
363 pseudomorphs and rare coesite relics documenting that they underwent UHP  
364 metamorphism, whereas multiple-phase needles in garnet show that the eclogites  
365 suffered UHP metamorphism with a possible pressure > 5–7 GPa. Other  
366 mineralogical and microtextural indicators, such as exsolved needles in clinopyroxene  
367 and F-apatite, are also present in the eclogite from the studied area and support peak  
368 UHP conditions.

369

## 370 *5.2. Factors helping the poor preservation of UHP traces*

371 Rapid exhumation for most UHP terranes has now been confirmed with  
372 geochronological data (e.g., Gebauer et al. 1997; Rubatto and Hermann 2001;  
373 Carswell et al. 2003; Mosenfelder et al., 2005 and references therein) and stable  
374 isotope data (Zheng et al., 2003). This geodynamic mechanism also help to some  
375 extent the preservation of coesite and related UHP phases. However, according to  
376 many authors (e.g., Liou and Zhang, 1996; Liou et al., 1997; Mosenfelder et al. 2005  
377 and references therein), the preservation of coesite and other UHP evidences may  
378 depend on many factors including the rigidity of the host mineral, the P-T conditions

379 and path of metamorphic crystallization, the rate of exhumation, continuous cooling  
380 during decompression, and prevention of fluid infiltration into the host mineral until  
381 fracturing at low temperatures or the presence of fluids during retrogression. Perhaps  
382 the most vital factor for the survival of coesite is its inclusion in strong host phases,  
383 such as garnet and zircon, which can act as “pressure vessels” and sustain an  
384 overpressure on the inclusion, inhibiting the volume increase necessary to transform it  
385 to quartz. That is to say, mineral inclusions in zircon or garnet may witness peak  
386 metamorphism or earlier stages of metamorphism (Chopin, 2003).

387 The petrologic observations described in this paper clearly reveal that the studied  
388 eclogites suffered a complex metamorphic evolution resulting in multistage  
389 decompression related to exhumation, which most likely obliterated almost all of the  
390 earlier evidence for coesite and UHP metamorphism. As a consequence, so far few  
391 evidence for UHP metamorphism has been found in the NDZ. The poor preservation  
392 of UHP conditions in the eclogites and orthogneisses of the NDZ might be also  
393 favored by the presence of partial melts during decompression from coesite- or  
394 diamond- to granulite-facies conditions as experimentally documented by Hermann et  
395 al. (2001), which is supported by the evidence for partial melting of the eclogites (Liu  
396 Y.-C. et al., unpublished data). Unfortunately, the textures of the orthogneisses cannot  
397 be used to prove this hypothesis because of their felsic composition and the  
398 subsequent, pervasive granulite- and amphibolite-facies overprint.

399 The P-T path followed by the eclogites of the NDZ (Fig. 7) maintained high- to  
400 very-high-temperature conditions for a long way from the early stages of uplift at

401 UHP conditions to HP granulite-facies overprinting. This peculiar P-T evolution,  
402 together with the influx of later abundant fluid circulation during the  
403 amphibolite-facies retrogression, may contribute to explain the extremely rare  
404 preservation of coesite and related UHP relics (Liou and Zhang, 1996; Mosenfelder et  
405 al., 2005). The early post-peak P-T history of the NDZ eclogites (Liu et al., 2000,  
406 2007a; Xu et al., 2000), allowed to retain equilibration temperatures exceeding 850 °C  
407 during exhumation up to lower crustal levels (1.1-1.4 GPa and 804–857 °C); the  
408 following evolution is marked by both temperature and pressure decrease (Fig. 7). In  
409 such a P-T path, characterized mainly by isothermal decompression, the difference  
410 between internal and external pressure of garnet reaches its maximum at the end of  
411 isothermal decompression, and garnet fracturing would occur at high temperatures (>  
412 800°C), leading to rapid diffusion (Nakano et al., 2007) and slow cooling with a  
413 complete breakdown of coesite (Ghiribelli et al., 2002; Faryad et al., 2010) or even  
414 the possibility that in most cases coesite would have been consumed (Tsai and Liou,  
415 2000) at such HT condition during the granulite-facies overprint.

416

### 417 *5.3. Implications for the exhumation of UHP rocks*

418 The data presented in this paper show that the eclogites from the Luotian dome in  
419 the NDZ experienced a multistage and relatively slow cooling process at high-T  
420 conditions after peak UHP metamorphism, with a widespread HP granulite-facies  
421 overprinting. In contrast, the CDZ and SDZ underwent rapid exhumation and cooling  
422 from the eclogite-facies to the amphibolite-facies metamorphic stage without any

423 granulite-facies overprinting. As a result, the eclogites in the NDZ are characterized  
424 by peculiar multiple decompression microtextures, and do not preserve almost any  
425 evidence of UHP metamorphism because of complete retrogression of UHP minerals  
426 due to action of fluids during the late amphibolite-facies overprinting and/or to the  
427 complete decomposition of coesite and related minerals during high-T exhumation.  
428 Therefore, the Dabie orogen comprises three eclogite-bearing terranes (i.e., the NDZ,  
429 CDZ and SDZ), all subjected to UHP metamorphism, characterized by different  
430 evolutionary processes and exhumation histories. This conclusion further supports the  
431 model for multi-slice and multistage successive exhumation of UHP metamorphic  
432 rocks proposed by Liu et al. (2007b).

433

## 434 **6. Conclusions**

435 The eclogites from the NDZ underwent a prolonged exhumation history from  
436 eclogite- via granulite- and amphibolite-facies conditions, resulting in the common  
437 formation of peculiar multistage decompression textures and the extremely rare  
438 preservation of former UHP metamorphic evidence. The studied eclogites were  
439 strongly affected by multiple recrystallization processes during exhumation, thus  
440 making the determination of peak metamorphic conditions particularly difficult.  
441 However, the occurrence of radial cracks around quartz inclusions and of  
442 polycrystalline quartz inclusions in garnet, most likely suggests that these inclusions  
443 formerly were coesite, now inverted to quartz. This hypothesis is also supported by  
444 the presence of relic coesite which has been confirmed by Raman spectroscopy.



445 Moreover, the occurrence of rutile + clinopyroxene + amphibole + apatite oriented  
446 needles in garnet open the possibility of peak pressure exceeding 5-7 GPa in the NDZ.  
447 An important consequence of this study is that if the eclogites from the Luotian dome  
448 suffered UHP metamorphism, they are perfectly comparable to those from the  
449 northeastern part of the NDZ; in this respect, the NDZ wholly experienced Triassic  
450 UHP metamorphism as a coherent unit.

451

## 452 **Acknowledgements**

453 This research was financially supported by the National Basic Research Program of  
454 China (2009CB825002), the National Natural Science Foundation of China  
455 (40921002, 40973043 and 40572035), the PhD Foundation of the Ministry of  
456 Education of China (200803580001) and the Chinese Academy of Sciences  
457 (kzcx2-yw-131). We would like to thank Prof. Shuguang Li for his valuable  
458 discussion and helpful suggestions on this study. The authors are also grateful to Ms.  
459 Ling Yan for the Raman analysis.

460

461 **References**

- 462 Ayers, J.C., Dunkle, S., Gao, S., Miller, C.F., 2002. Constraints on timing of peak and  
463 retrograde metamorphism in the Dabie Shan ultrahigh-pressure metamorphic belt,  
464 east-central China, using U-Th-Pb dating of zircon and monazite. *Chemical*  
465 *Geology* 186, 315–331.
- 466 Boyer, H., Smith, D.C., Chopin, C., Lasnier, B., 1985. Raman microprobe (RMP)  
467 determinations of natural and synthetic coesite. *Physics and Chemistry of*  
468 *Minerals* 12, 45–48.
- 469 Bryant, J.L., Ayers, J.C., Gao, S., Miller, C.F., Zhang, H., 2004. Geochemical, age,  
470 and isotopic constrains on the location of the Sino-Korean/Yangtze suture and  
471 evolution of the Northern Dabie Complex, east central China. *Geological Society*  
472 *of America Bulletin* 116, 698–717.
- 473 Carswell, D.A., Brueckner, H.K., Cuthbert, S.J., Mehta, K., O'Brien, P.J., 2003. The  
474 timing of stabilisation and the exhumation rate for ultra-high pressure rocks in the  
475 Western Gneiss Region of Norway. *Journal of Metamorphic Geology* 21,  
476 601–612.
- 477 Chavagnac, V., Jahn, B.M., 1996. Coesite-bearing eclogites from the Bixiling complex.  
478 Dabie Mountains, China: Sm–Nd ages, geochemical characteristics and tectonic  
479 implications. *Chemical Geology* 133, 29–51.
- 480 Chopin, C., 1984. Coesite and pure pyrope in high-grade blue schists of the western  
481 Alps: a first record and some consequences. *Contributions to Mineralogy and*  
482 *Petrology* 86, 107–118.

483 Chopin, C., Sobolev, N.V., 1995. Principal mineralogical indicators of UHP in crustal  
484 rocks, in: Coleman R.G. and Wang X. (eds), Ultrahigh pressure metamorphism,  
485 Cambridge University Press, pp. 96–133.

486 Chopin, C., 2003. Ultrahigh-pressure metamorphism: tracing continental crust into the  
487 mantle. *Earth and Planetary Science Letters* 212, 1–14.

488 Dobrzhinetskaya, L., Schweinehage, R., Massonne, H.J., Green, H.W., 2002. Silica  
489 precipitates in omphacite from eclogite at Alpe Arami, Switzerland: evidence of  
490 deep subduction. *Journal of Metamorphic Geology* 20, 481–492.

491 Faryad, S.W., 2009. The Kutná Hora Complex (Moldanubian zone, Bohemian Massif):  
492 A composite of crustal and mantle rocks subducted to HP/UHP conditions. *Lithos*  
493 109, 193–208.

494 Faryad, S.W., Nahodilová, R., Dolejš, D., 2010. Incipient eclogite facies  
495 metamorphism in the Moldanubian granulites revealed by mineral inclusions in  
496 garnet. *Lithos* 114, 54–69.

497 Gasparik, T., 1986. Experimental study of subsolidus phase relations and mixing  
498 properties of clinopyroxene in silica-saturated system CaO-MgO-Al<sub>2</sub>O<sub>3</sub>-SiO<sub>2</sub>.  
499 *American Mineralogist* 71, 686–693.

500 Gayk, T., Kleinschrodt, R., Langosch, A., Seidel, E., 1995. Quartz exsolution in  
501 clinopyroxene of high-pressure granulite from the Munchberg Massif. *European*  
502 *Journal of Mineralogy* 7, 1217–1220.

503 Gebauer, D., Schertl, H.-P., Brix, M., Schreyer, W., 1997. 35 Ma old  
504 ultrahigh-pressure metamorphism and evidence for very rapid exhumation in the

505 Dora Maira massif, Western Alps. *Lithos* 41, 5–24.

506 Ghiribelli, B., Frezzotti, M.-L., and Palmeri, R., 2002. Coesite in eclogites of the  
507 Lanterman Range (Antarctica): Evidence from textural and Raman studies.  
508 *European Journal of Mineralogy* 14, 355–360.

509 Hacker, B.R., Ratschbacher, L., Webb, L.E., Ireland, T.R., Walker, D., Dong, S., 1998.  
510 U/Pb zircon ages constrain the architecture of the ultrahigh-pressure  
511 Qinling-Dabie orogen, China. *Earth and Planetary Science Letters* 161, 215–230.

512 Harley, S.L., 1998. On the occurrence and characterization of ultrahigh-temperature  
513 (UHT) crustal metamorphism. In: *What Controls Metamorphism and*  
514 *Metamorphic Reactions?* In: Treloar, P.J., O'Brien, P. (eds.), Special Publication  
515 *Geological Society of London* 138, 75–101.

516 Hermann, J., Rubatto, D., Korsakov, A., and Shatsky, V.S., 2001. Multiple zircon  
517 growth during fast exhumation of diamondiferous, deeply subducted continental  
518 crust (Kokchetav massif, Kazakhstan). *Contributions to Mineralogy and*  
519 *Petrology* 141, 66–82.

520 Katayama, I., Parkinson, C.D., Okamoto, K., Nakajima, Y., Maruyama, S., 2000a.  
521 Supersilicic clinopyroxene and silica exsolution in UHPM eclogite and pelitic  
522 gneiss from the Kokchetav massif, Kazakhstan. *American Mineralogist*, 85,  
523 1368–1374.

524 Katayama, I., Zayachkovsky, A.A., Maruyama, S., 2000b. Prograde  
525 pressure-temperature records from inclusions in zircons from ultrahigh-pressure –  
526 high-temperature rocks of the Kokchetav Massif, northern Kazakhstan. *Island Arc*

527 9, 417–427.

528 Korsakov, A.V., Perraki, M., Zhukov, V.P., Gussem, K.D., Vandenabeele, P.,  
529 Tomilenko, A.A., 2009. Is quartz a potential indicator of ultrahigh-pressure  
530 metamorphism? Laser Raman spectroscopy of quartz inclusions in  
531 ultrahigh-pressure garnets. *European Journal of Mineralogy* 21, 1313–1323.

532 Kretz, R., 1983. Symbols for rock-forming mineral. *American Mineralogist* 68,  
533 277–279.

534 Li, S., Xiao, Y., Liu, D., Chen, Y., Ge, N., Zhang, Z., Sun, S. S., Cong, B., Zhang, R.,  
535 Hart, S.R., Wang, S., 1993. Collision of the North China and Yangtze blocks and  
536 formation of coesite-bearing eclogites: timing and processes. *Chemical Geology*  
537 109, 89–111.

538 Li S., Jagoutz E., Chen Y., Li Q., 2000. Sm-Nd and Rb-Sr isotope chronology of  
539 ultrahigh-pressure metamorphic rocks and their country rocks at Shuanghe in the  
540 Dabie Mountains, central China. *Geochimica Cosmochimica Acta* 64, 1077–1093.

541 Li, S., Huang, F., Zhou, H., Li, H., 2003. U-Pb isotopic compositions of the ultrahigh  
542 pressure metamorphic (UHPM) rocks from Shuanghe and gneisses from Northern  
543 Dabie zone in the Dabie Mountains, central China: Constraint on the exhumation  
544 mechanism of UHPM rocks. *Science in China (Series D)* 46, 200–209.

545 Li, X.-P., Zheng, Y.-F., Wu, Y.-B., Chen, F.K., Gong, B., Li, Y.-L., 2004. Low-T  
546 eclogite in the Dabie terrane of China: petrological and isotopic constrains on  
547 fluid activity and radiometric dating. *Contributions to Mineralogy and Petrology*  
548 148, 443–470.

549 Liou, J.G., Zhang, R.Y., 1996. Occurrences of intergranular coesite in ultrahigh-P  
550 rocks from the Sulu region, eastern China: implications for lack of fluid during  
551 exhumation. *American Mineralogist* 81, 1217–1221.

552 Liou, J.G., Zhang, R.Y., Jahn, B.M., 1997. Petrology, geochemistry and isotope data  
553 on a ultrahigh-pressure jadeite quartzite from Shuanghe, Dabie Mountains,  
554 east-central China. *Lithos* 41, 50–78.

555 Liou, J. G., Zhang, R. Y., Ernst, W. G., Rumble, D., Maruyama, S., 1998.  
556 High-pressure minerals from deeply subducted metamorphic rocks. *Review of*  
557 *Mineralogy* 37, 33–96.

558 Liu, F.L., Xu, Z.Q., Liou, J.G., Katayama, I., Masago, H., Maruyama, S., Yang, J.,  
559 2002. Ultrahigh-pressure mineral inclusions in zircons from gneissic core samples  
560 of the Chinese Continental Scientific Drilling Site in eastern China. *European*  
561 *Journal of Mineralogy* 14, 499–512.

562 Liu, J.B., Ye, K., Maruyama, S., Cong, B.L., Fa, H.R., 2001. Mineral inclusions in  
563 zircon from gneisses in the ultrahigh-pressure zone of the Dabie Mountains,  
564 China. *The Journal of Geology* 109, 523–535.

565 Liu, Y.-C., Li, S., Xu, S., Li, H., Jiang, L., Chen, G., Wu, W., Su, W., 2000. U-Pb  
566 zircon ages of the eclogite and tonalitic gneiss from the northern Dabie  
567 Mountains, China and multi-overgrowths of metamorphic zircons. *Geological*  
568 *Journal of China Universities* 6, 417–423 (in Chinese with English abstract).

569 Liu, Y.-C., Li, S., Xu, S., Jahn, B.-M., Zheng, Y., Zhang, Z., Jiang, L., Chen, G., Wu,  
570 W., 2005. Geochemistry and geochronology of eclogites from the northern Dabie

571 Mountains, central China. *Journal of Asian Earth Sciences* 25, 431–443.

572 Liu, Y.-C., Li, S., Gu, X., Xu, S., Chen, G., 2007a. Ultrahigh-pressure eclogite  
573 transformed from mafic granulite in the Dabie orogen, east-central China. *Journal*  
574 *of Metamorphic Geology* 25, 975–989.

575 Liu, Y.-C., Li, S., Xu, S., 2007b. Zircon SHRIMP U-Pb dating for gneiss in northern  
576 Dabie high T/P metamorphic zone, central China: Implication for decoupling  
577 within subducted continental crust. *Lithos* 96, 170–185.

578 Liu, Y.-C., Li, S., 2008. Detachment within subducted continental crust and  
579 multi-slice successive exhumation of ultrahigh-pressure metamorphic rocks:  
580 Evidence from the Dabie-Sulu orogenic belt. *Chinese Science Bulletin* 53,  
581 3105–3119.

582 Liu, Y.-C., Wang, A., Rolfo, F., Groppo, C., Gu, X., Song, B., 2009. Geochronological  
583 and petrological constraints on Palaeoproterozoic granulite facies metamorphism  
584 in southeastern margin of the North China Craton. *Journal of Metamorphic*  
585 *Geology* 27, 125–138.

586 Liu, Y.-C., Gu, X., Li, S., Hou, Z., Song, B., 2010. Multistage metamorphic events in  
587 eclogites from the North Dabie high-T/UHP Complex zone, central China:  
588 evidence from zircon U-Pb age, trace element and mineral inclusion. Submitted.

589 Malaspina, N., Hermann, J., Scambelluri, M., Compagnoni, R., 2006. Multistage  
590 metasomatism in ultrahigh-pressure mafic rocks from the North Dabie Complex  
591 (China). *Lithos* 90, 19–42.

592 Mao, H.K., 1971. The system jadeite (NaAlSi<sub>2</sub>O<sub>6</sub>)-anorthite (CaAl<sub>2</sub>Si<sub>2</sub>O<sub>8</sub>) at high

593 pressure. Carnegie Institute Year Book 69, 163–168.

594 Mosenfelder, J.L., Bohlen, S.R., 1997. Kinetics of the coesite to quartz transformation.  
595 Earth and Planetary Science Letters 153, 133–147.

596 Mosenfelder, J.L., Schertl, H.-P., Smyth, J.R., Liou, J.G., 2005. Factors in the  
597 preservation of coesite: The importance of fluid infiltration. American  
598 Mineralogist 90, 779–789.

599 Mposkos, E.D., Kostopoulos, D.K., 2001. Diamond, former coesite and supersilicic  
600 garnet in metasedimentary rocks from the Greek Rhodope: a new  
601 ultrahigh-pressure metamorphic province established. Earth and Planetary  
602 Science Letters 192, 497–506.

603 Nakano, N., Osanai, Y, Owada, M., 2007. Multiple breakdown and chemical  
604 equilibrium of silicic clinopyroxene under extreme metamorphic conditions in the  
605 Kontum Massif, central Vietnam. American Mineralogist 92, 1844–1855.

606 Okay, A.I., Xu S., Sengör, A.M.C., 1989. Coesite from the Dabie Shan eclogites,  
607 central China. European Journal of Mineralogy 1, 595–598.

608 Okay, A.I., 1993. Petrology of a diamond and coesite-bearing metamorphic terrain:  
609 Dabie Shan, China. European Journal of Mineralogy 5, 659–675.

610 Okay, A.I., Sengör, A.M.C., Satir, M., 1993. Tectonics of an ultrahigh-pressure  
611 metamorphic terrane: the Dabie Shan/Tongbai orogen, China. Tectonics 12,  
612 1320–1334.

613 Page, F.Z., Essene, E.J., Mukasa, S.B., 2005. Quartz exsolution in clinopyroxene is  
614 not proof of ultrahigh pressures: Evidence from eclogites from the Eastern Blue



615 Ridge, Southern Appalachians, U.S.A. *American Mineralogist* 90, 1092–1099.

616 Parkinson, C. D., Katayama, I., 1999. Present day ultrahigh-pressure conditions of  
617 coesite inclusions in zircon and garnet: evidence from laser Raman  
618 microspectroscopy. *Geology* 27, 979–982.

619 Perrillat, J.P., Daniel, I., Lardeaux, J.M., Cardon, H., 2003. Kinetics of the  
620 coesite–quartz transition: application to the exhumation of ultrahigh-pressure  
621 rocks. *Journal of Petrology*, 44, 773–788.

622 Rolfo, F., Compagnoni, R., Xu, S., Jiang, L., 2000. First report of felsic whiteschist in  
623 the ultrahigh-pressure metamorphic belt of Dabie Shan, China. *European Journal*  
624 *of Mineralogy* 12, 883–898.

625 Rolfo, F., Compagnoni, R., Wu, W., Xu, S., 2004. A coherent lithostratigraphic unit in  
626 the coesite-eclogite complex of Dabie Shan, China: geologic and petrologic  
627 evidence. *Lithos* 73, 71–94.

628 Rubatto, D., Hermann, J., 2001. Exhumation as fast as subduction? *Geology* 29, 3–6.

629 Smith, D.C., 1984. Coesite in clinopyroxene in the Caledonides and its implications  
630 for geodynamics. *Nature* 310, 641–644.

631 Song, S.G., Yang, J.S., Xu, Z.Q., Liou, J.G., Shi, R.D., 2003. Metamorphic evolution  
632 of the coesite-bearing ultrahigh-pressure terrane in the North Qaidam, northern  
633 Tibet, NW China. *Journal of Metamorphic Geology* 21, 631–644.

634 Song, S.G., Zhang, L., Chen, J., Liou, J.G., Niu, Y., 2005. Sodic amphibole exsolutions  
635 in garnet from garnet-peridotite, North Qaidam UHPM belt, NW China:  
636 Implications for ultradeep-origin and hydroxyl defects in mantle garnets.

637 American Mineralogist 90, 814–820.

638 Spear, F.S., Pyle, J.M., 2002. Apatite, Monazite, and Xenotime in metamorphic rocks.  
639 Reviews in Mineralogy and Geochemistry 48, 293–335.

640 Tabata, H., Yamauchi, K., Maruyama, S., Liou J.G., 1998. Tracing the extent of a UHP  
641 metamorphic terrane: Mineral-inclusion study of zircons in gneisses from the  
642 Dabieshan, In: B.R. Hacker, J.G. Liou (eds.), When Continents Collide:  
643 Geodynamics and Geochemistry of Ultrahigh-Pressure Rocks. Kluwer Academic  
644 Publisher, pp. 261–273.

645 Tsai, C.H., Liou, J.G., 2000. Eclogite-facies relics and inferred ultrahigh-pressure  
646 metamorphism in the North Dabie complex, central China. American Mineralogist  
647 85, 1–8.

648 Wang, X., Liou, J.G., Mao, H.K., 1989. Coesite-bearing eclogites from the Dabie  
649 Mountains in central China. Geology 17, 1085–1088.

650 Wells, R.A., 1977. Pyroxene thermometry in simple and complex systems.  
651 Contributions to Mineralogy and Petrology 62, 129–139.

652 Wood, B.J., Banno, S., 1973. Garnet-orthopyroxene and orthopyroxene-clinopyroxene  
653 relationship in simple and complex systems. Contributions to Mineralogy and  
654 Petrology 42, 109–124.

655 Wood, B.J., Henderson, C.M.B., 1978. Compositions and unit-cell parameters of  
656 synthetic non-stoichiometric tschermakitic clinopyroxenes. American  
657 Mineralogist 63, 66–72.

658 Xu, S., Okay, A.I., Ji, S., Sengör, A.M.C., Su, W., Liu, Y., Jiang, L., 1992. Diamond

659 from the Dabie Shan metamorphic rocks and its implication for tectonic setting.  
660 Science 256, 80–82.

661 Xu, S., Liu, Y.-C., Su, W., Wang, R., Jiang, L., Wu, W., 2000. Discovery of the  
662 eclogite and its petrography in the Northern Dabie Mountains. Chinese Science  
663 Bulletin 45, 273–278.

664 Xu, S., Liu, Y.-C., Chen, G., Compagnoni, R., Rolfo, F., He, M., Liu, H., 2003. New  
665 finding of micro-diamonds in eclogites from Dabie-Sulu region in central-eastern  
666 China. Chinese Science Bulletin 48, 988–994.

667 Xu, S., Liu, Y.-C., Chen, G., Ji, S., Ni, P., Xiao, W., 2005, Microdiamonds, their  
668 classification and tectonic implications for the host eclogites from the Dabie and  
669 Su-Lu regions in central eastern China. Mineralogical Magazine 69, 509–520.

670 Ye K., Cong B., Ye D., 2000a. The possible subduction of continental material to  
671 depths greater than 200 km. Nature 407, 734–736.

672 Ye, K., Yao, Y., Katayama, I., Cong, B., Wang, Q., Maruyama. S., 2000b. Large areal  
673 extent of ultrahigh-pressure metamorphism in the Sulu ultrahigh-pressure terrane  
674 of East China: new implications from coesite and omphacite inclusions in zircon  
675 of granitic gneiss. Lithos 52, 157–164.

676 Zhang, H., Gao, S., Zhong, Z., Zhang, B., Zhang, L., Hu, S., 2002a. Geochemical and  
677 Sr–Nd–Pb isotopic compositions of Cretaceous granitoids: constraints on tectonic  
678 framework and crustal structure of the Dabieshan ultrahigh-pressure metamorphic  
679 belt, China. Chemical Geology 186, 281–299.

680 Zhang L., Ellis D.J., Jiang W., 2002b. Ultrahigh pressure metamorphism in western

681 Tianshan, China, part I: evidences from the inclusion of coesite pseudomorphs in  
682 garnet and quartz exsolution lamellae in omphacite in eclogites. *American*  
683 *Mineralogist* 87, 853–860.

684 Zhang, L.F., Song, S., Liou, J.G., Ai, Y., Li, X., 2005. Relict coesite exsolution in  
685 omphacite from Western Tianshan eclogites, China: *American Mineralogist* 90,  
686 181–186.

687 Zhang, R.Y., Hirajima, T., Banno, S., Cong, B., Liou, J.G., 1995. Petrology of  
688 ultrahigh pressure rocks from the southern Sulu region, eastern China. *Journal of*  
689 *Metamorphic Geology* 13, 659–675.

690 Zhang, R.Y., Zhai, S.M., Fei, Y.W., Liou, J.G., 2003. Titanium solubility in coexisting  
691 and clinopyroxene at very high pressure: the significance of exsolved rutile in  
692 garnet. *Earth and Planetary Science Letters* 216, 591–601.

693 Zhang, R.Y., Liou, J.G., Ernst, W.G., 2009. The Dabie–Sulu continental collision zone:  
694 A comprehensive review. *Gondwana Research* 16, 1–26.

695 Zhao, Z., Zheng, Y., Wei, C., Chen, F., Liu, X., Wu, F., 2008. Zircon U–Pb ages, Hf  
696 and O isotopes constrain the crustal architecture of the ultrahigh-pressure Dabie  
697 orogen in China. *Chemical Geology* 253, 222–242.

698 Zharikov, V.A., Ishbulatov, R.A., Chudinovskikh, L.T., 1984. High-pressure  
699 clinopyroxenes and eclogite barrier. *Soviet Geology and Geophysics* 25, 53–61.

700 Zheng, Y., Fu, B., Gong, B., Li, L., 2003. Stable isotope geochemistry of ultrahigh  
701 pressure metamorphic rocks from the Dabie-Sulu orogen in China: implications  
702 for geodynamics and fluid regime. *Earth Science Reviews* 62, 105–161.

703

704 **Figure captions**

705 **Figure 1** Schematic geological map of the Dabie orogen. Sample localities with  
706 sample numbers are described in detail in the text. BZ = Beihuaiyang zone, NDZ =  
707 North Dabie complex zone, CDZ = Central Dabie UHP metamorphic zone, SDZ =  
708 South Dabie low-T eclogite zone, SZ = Susong complex zone, HMZ = Huwan  
709 mélange zone, HZ = Hong'an low-T eclogite zone, DC = amphibolite-facies Dabie  
710 complex, XMF= Xiaotian-Mozitan fault, WSF= Wuhe-Shuihou fault, HMF =  
711 Hualiangting-Mituo fault, TSF= Taihu-Shanlong fault, TLF = Tan-Lu fault. The inset  
712 shows the location of Fig. 1 within the Triassic Qinling—Dabie—Su-Lu collision  
713 orogen in central China.

714

715 **Figure 2** Field occurrence of eclogite band (a) and lens (b) from the Luotian dome in  
716 the southwestern part of the North Dabie complex zone.

717

718 **Figure 3** Photomicrographs of eclogite from the Luotian dome in the Dabie orogen. a.  
719 Omphacite inclusion in garnet with two generations of symplectites (Hy+Di+Pl and  
720 Hbl+Pl+Mt), sample 06LT4-2; b. Omphacite, rutile and quartz inclusions in garnet,  
721 rimmed by distinctive double symplectites, sample 07LT6-1; c. quartz inclusion in  
722 garnet with well-developed radial fractures, sample 07LT6-1; d. Apatite (Ap) occurs  
723 as inclusion in garnet and in the matrix, the former is fluor-apatite (F-Ap) and the  
724 latter contains oriented pyrrhotite exsolutions (Po), sample 06LT4-2.

725

726 **Figure 4** Photomicrographs (a and d–f) and Back scattered electron (BSE) images (b  
727 and c) of eclogite from the Luotian dome showing multiple decompression textures. a.  
728 Diopside inclusion with quartz rods in garnet, sample 03LT1-1; b. Qtz + Pl + Hbl +  
729 Hy oriented needles in clinopyroxene, sample 03LT8-1; c. Qtz + Hy oriented needles  
730 in clinopyroxene, sample 06LT3-2; d. Cpx + Rt + Hbl + Ap oriented needles in garnet,  
731 sample 03LT1-1; e. Quartz after coesite in garnet, sample 09LT2-1; f. Cross-polarized  
732 light image of (e), showing polycrystalline quartz inclusions in garnet.

733

734 **Figure 5** a. Photomicrograph showing needle pyrrhotite (Po) exsolutions in apatite  
735 (Ap) and Cpx with quartz needles, sample 06LT3-2; b. The EDS spectra of exsolution  
736 rods in apatite from (a).

737

738 **Figure 6** Photomicrographs (a and b) of coesite (Cs) and quartz (Qtz) inclusion in  
739 zircon (Zr) and their mixed Raman spectra (c); zircon separated from the eclogite  
740 sample 03LT1-1 from the Luotian dome. The black circle in (a) is LA-ICPMS dating  
741 analysis with available  $^{206}\text{Pb}/^{208}\text{U}$  age shown.

742

743 **Figure 7** Multistage exhumation P-T trajectory of the NDZ eclogites, based on  
744 available data from the north-eastern portion of the NDZ (Malapina et al., 2006) and  
745 from the Luotian dome (Liu et al., 2007a).

746

747 **Table captions**

748 Table 1 Electron microprobe analyses of representative minerals from the eclogites in  
749 the Luotian dome (wt%)

Figure 1  
[Click here to download high resolution image](#)

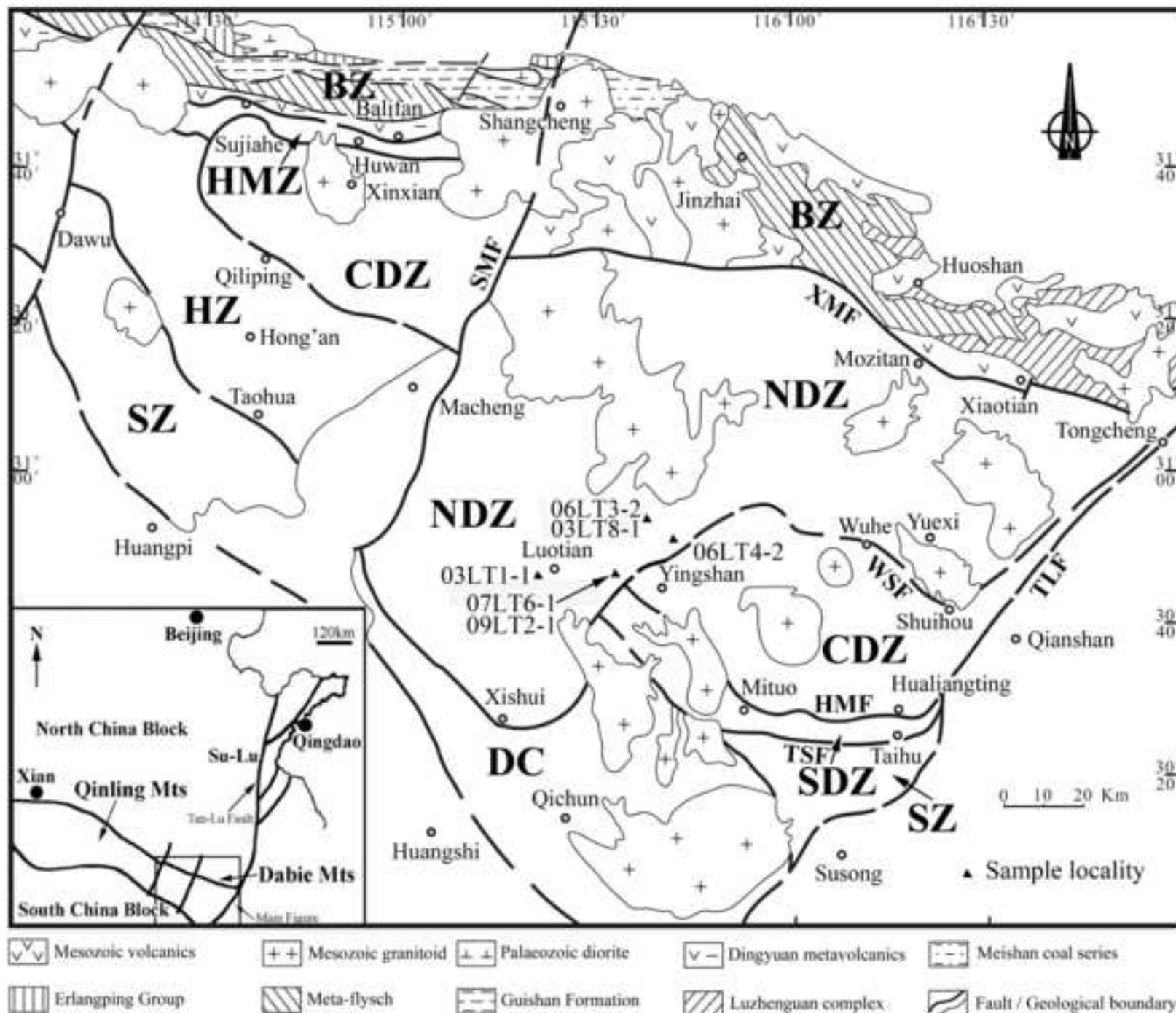


Figure 1



Figure 2  
[Click here to download high resolution image](#)



Figure 2



Figure 3  
[Click here to download high resolution image](#)

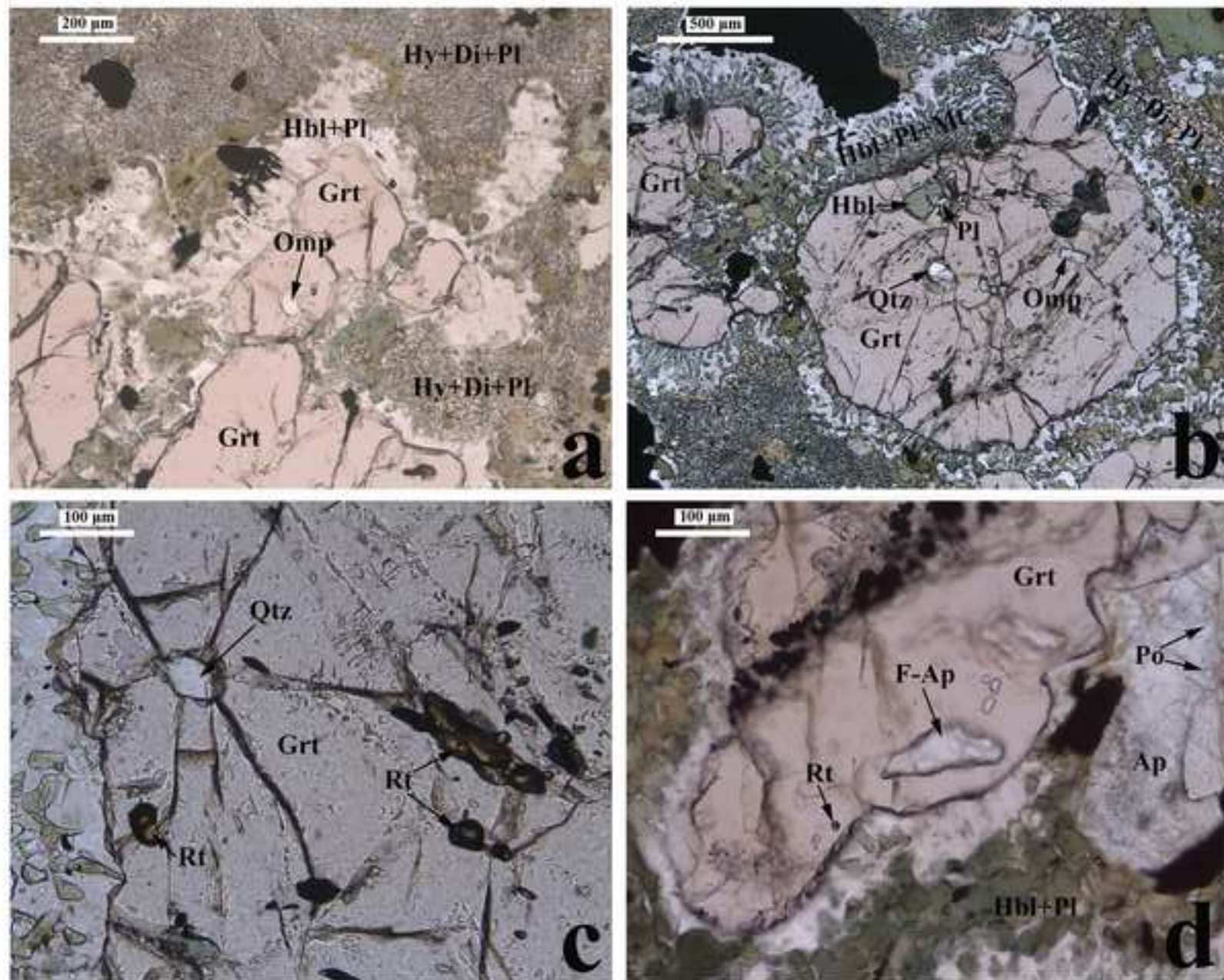


Figure 3

Figure 4  
[Click here to download high resolution image](#)

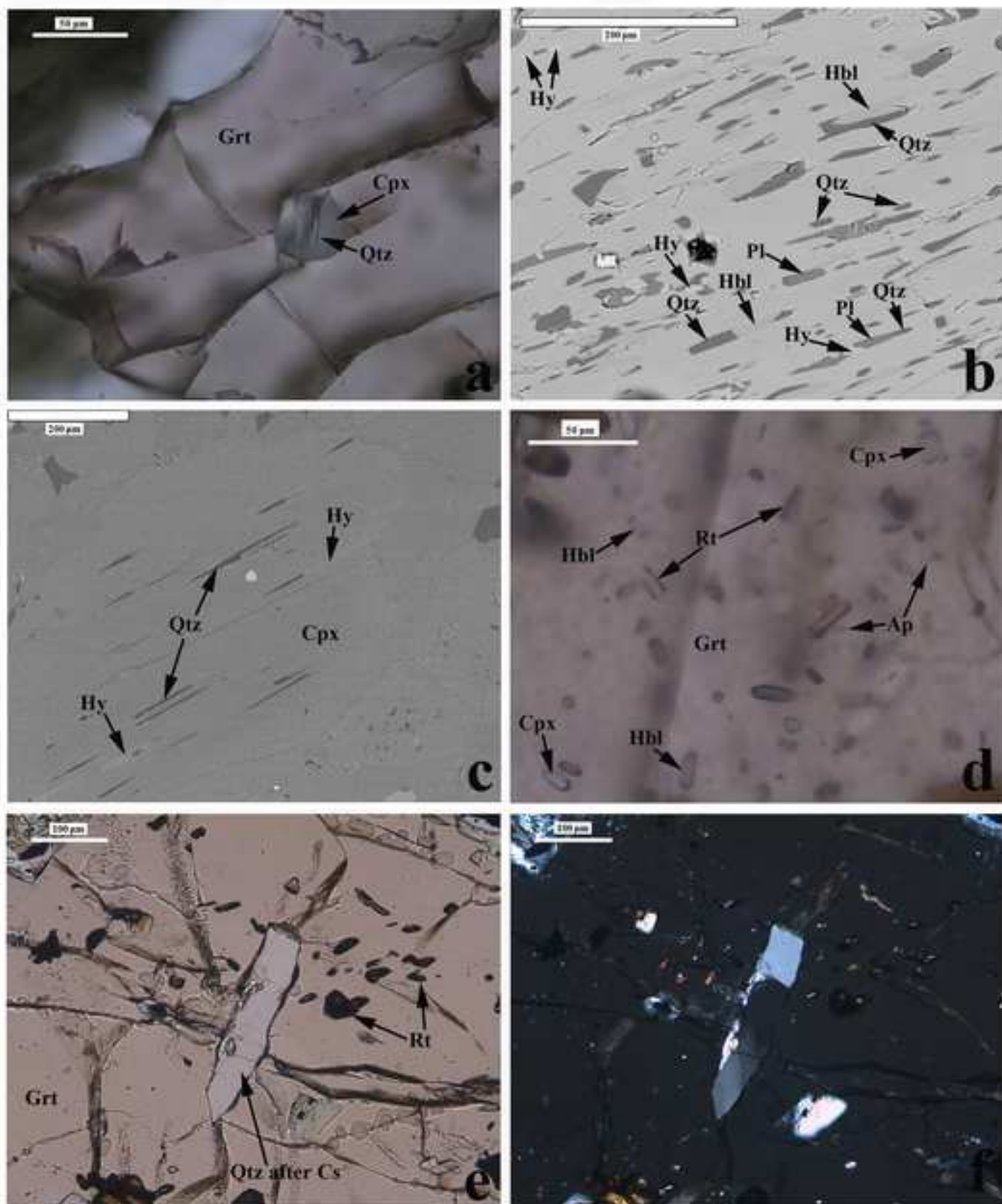


Figure 4



Figure 5  
[Click here to download high resolution image](#)

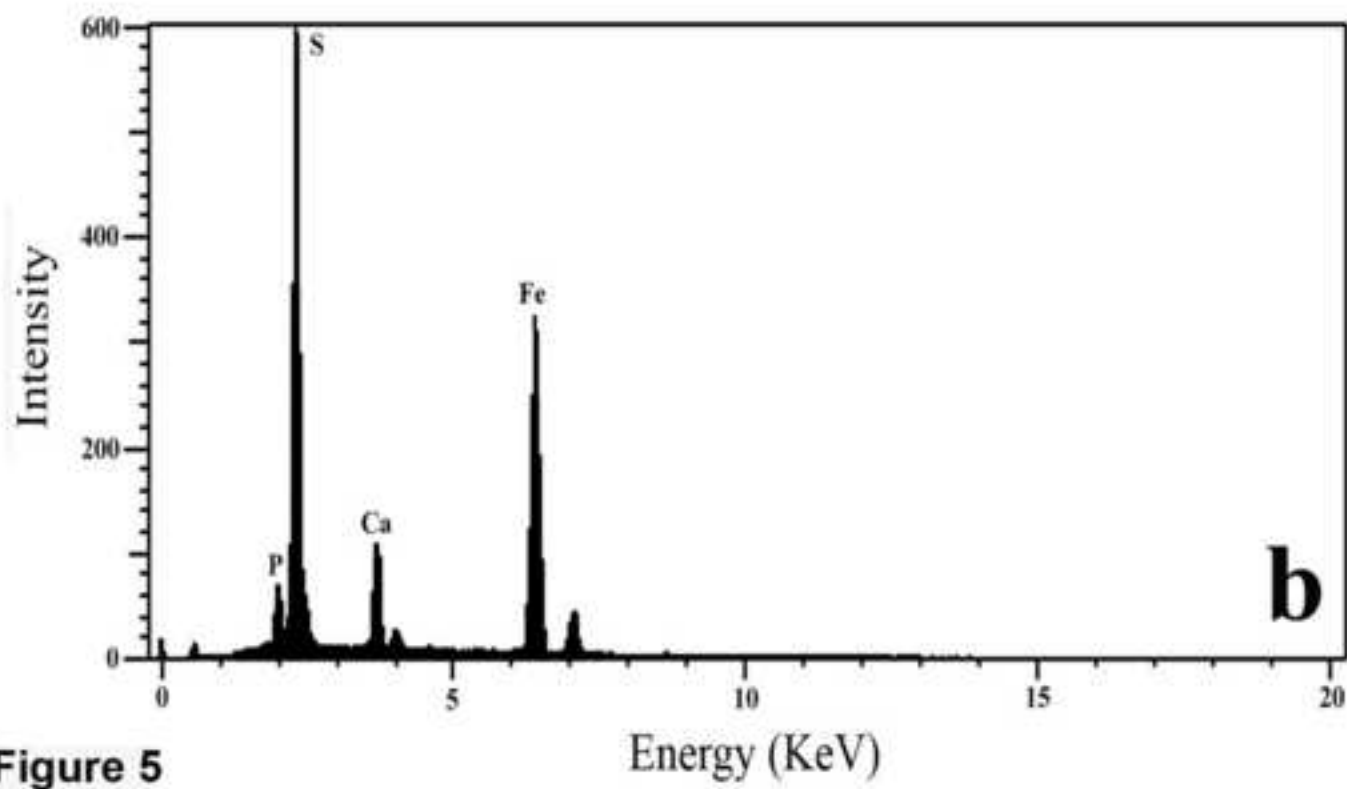
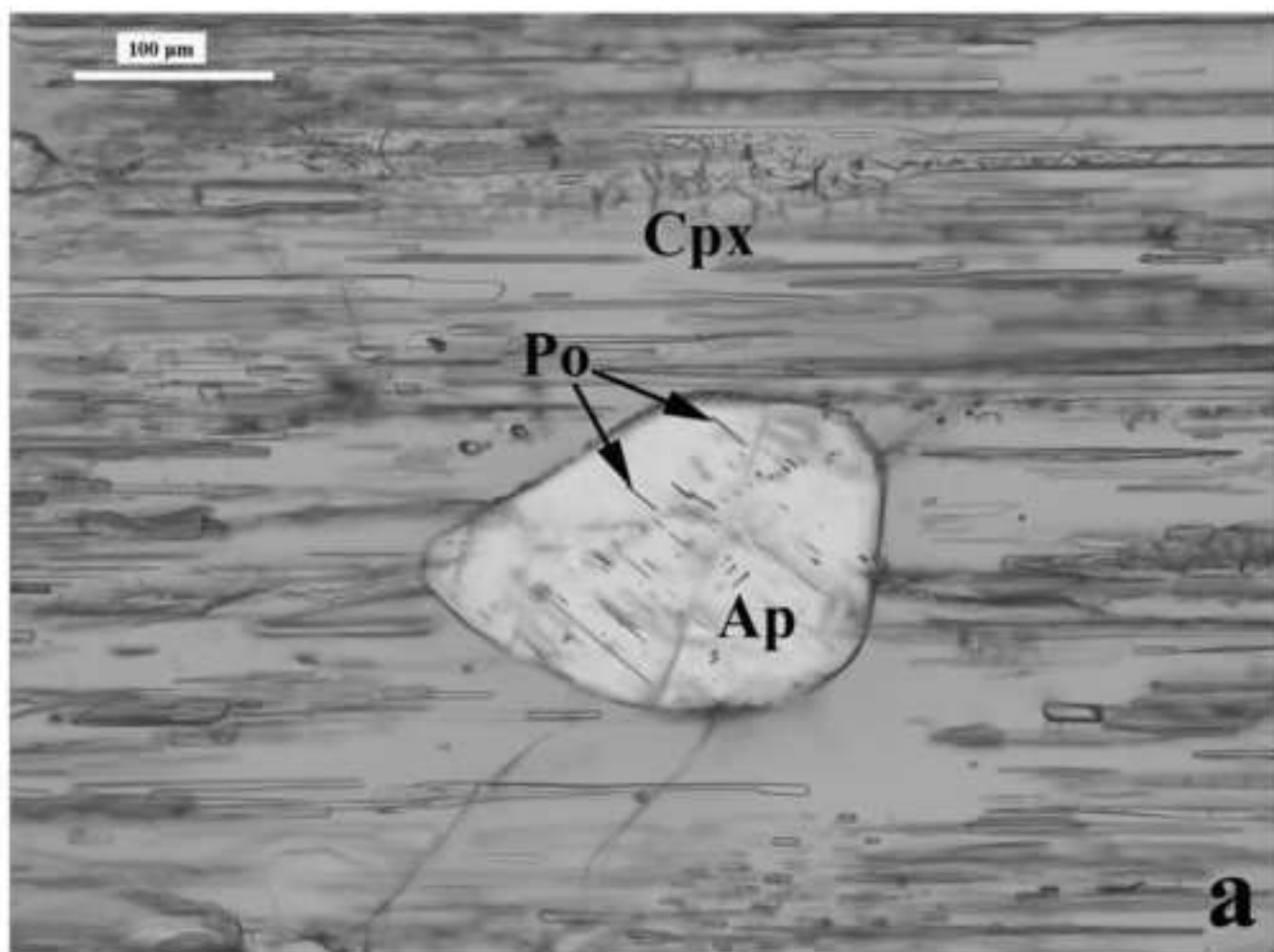


Figure 5

Figure6  
[Click here to download high resolution image](#)

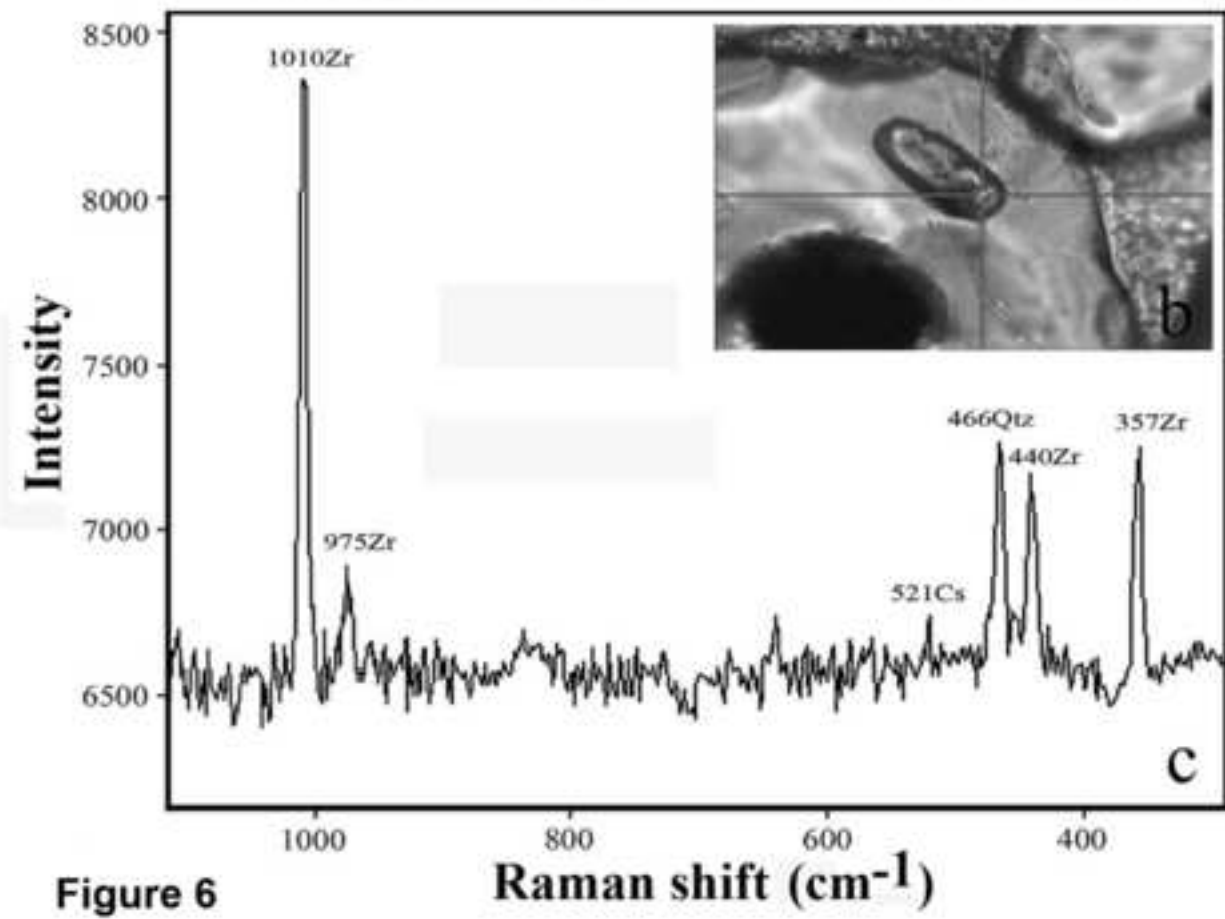
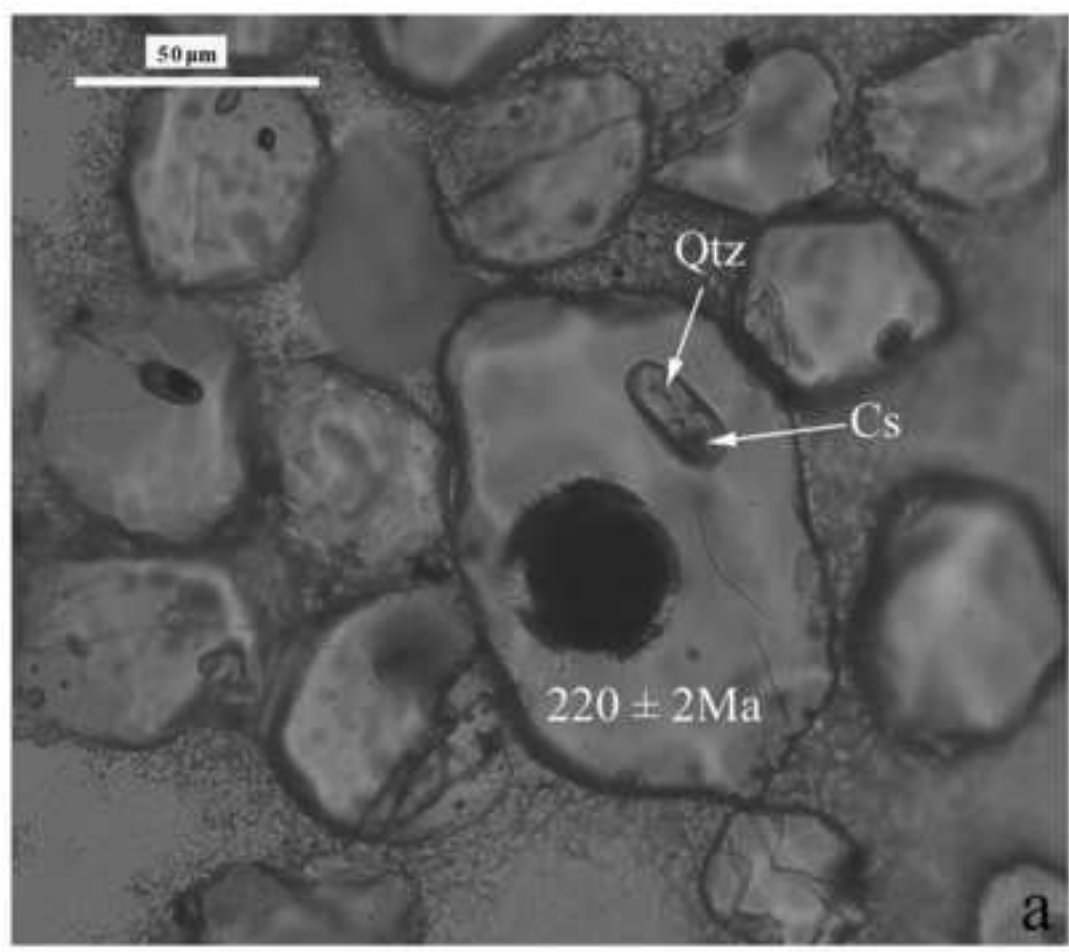


Figure 6

Raman shift (cm<sup>-1</sup>)

Figure 7

[Click here to download high resolution image](#)

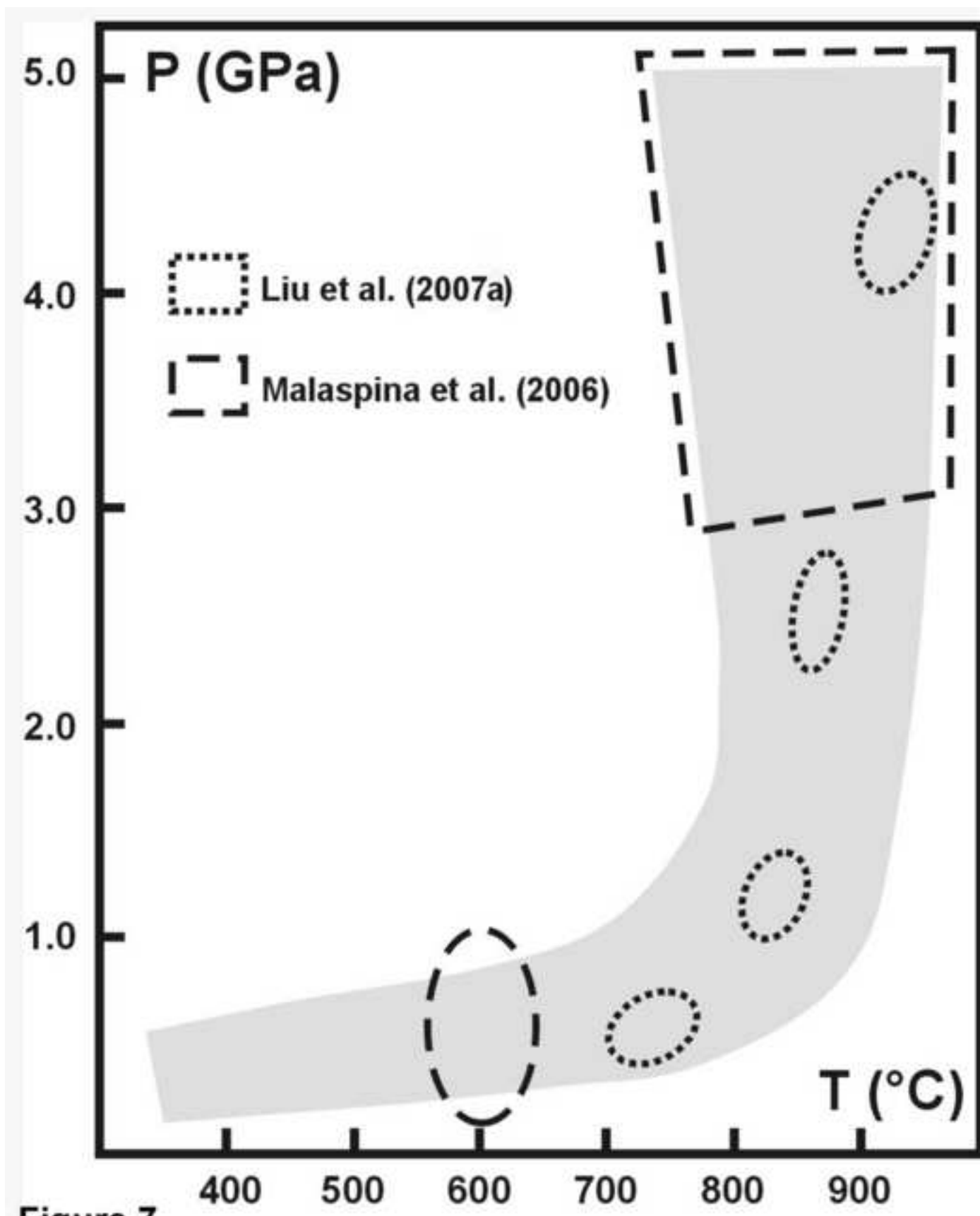


Figure 7

Table 1

Mineral	Garnet		Omphacite		Diopside	Hornblende		Plagioclase	
	No.	06LT3-2	06LT4-2	06LT3-2	06LT4-2	06LT3-2	06LT3-2	06LT3-2	03LT1-1
Locality	m	m	i	i	ng	nc	ng	nc	nc
<b>SiO<sub>2</sub></b>	38.88	38.43	54.45	55.28	52.7	45.12	38.65	61.2	61.46
<b>TiO<sub>2</sub></b>	0.02	0.07	0	0.04	0.1	0.08	0.73	0	0
<b>Al<sub>2</sub>O<sub>3</sub></b>	21.24	21.88	4.84	11.03	3.5	12.21	18.36	24.11	23.55
<b>FeO</b>	24.1	24.84	6.15	6.86	6.38	9.2	12.07	0	0.23
<b>Cr<sub>2</sub>O<sub>3</sub></b>	0	0	0.02	0	0.04	0.04	0	0	0
<b>MnO</b>	0.52	0.38	0.02	0.02	0.05	0.04	0.02	0.24	0.02
<b>MgO</b>	8.14	5.78	12.71	7.38	14.05	15.13	11.45	0	0.01
<b>CaO</b>	7.07	8.91	18.34	12.24	22.28	11.53	11.39	5.7	4.92
<b>Na<sub>2</sub>O</b>	0	0.12	2.95	7.33	0.83	2.27	2.89	8.71	9.05
<b>K<sub>2</sub>O</b>	0	0	0	0.01	0.01	0.03	0.02	0.01	0.02
<b>Total</b>	99.97	100.41	99.48	100.19	99.94	95.65	95.58	99.97	99.26
<b>O</b>	12	12	6	6	6	23	23	8	8
<b>Si</b>	2.985	2.964	1.986	1.967	1.938	6.526	5.71	2.723	2.749
<b>Al<sup>IV</sup></b>	0.015	0.036	0.014	0.033	0.062	1.474	2.29	1.263	1.241
<b>Al<sup>VI</sup></b>	1.905	1.951	0.194	0.430	0.09	0.606	0.904		
<b>Fe<sup>3+</sup></b>	0.102	0.09	0.028	0.106	0.025	0.626	0.787	0	0
<b>Ti</b>	0.001	0.004	0.000	0.001	0.003	0.009	0.081	0	0
<b>Fe<sup>2+</sup></b>	1.445	1.512	0.160	0.098	0.171	0.484	0.704	0.009	0.009
<b>Cr</b>	0	0	0.001	0	0.001	0.005	0	0	0
<b>Mg</b>	0.932	0.664	0.691	0.392	0.77	3.263	2.522	0	0.001
<b>Mn</b>	0.034	0.025	0.001	0.001	0.002	0.005	0.003	0	0.001
<b>Ca</b>	0.581	0.736	0.717	0.467	0.878	1.787	1.803	0.272	0.236
<b>Na</b>	0	0.018	0.209	0.506	0.059	0.637	0.828	0.751	0.785
<b>K</b>	0	0	0	0	0	0.006	0.004	0.001	0.001

Note: m, matrix; ng, oriented needle in garnet; nc, oriented needle in clinopyroxene; i, inclusion; sy, symplectite.

Continued Table 1

Mineral	Apatite		Diopside		Hypersthene		Hornblende	Plagioclase	
	No.	06LT3-2	06LT4-2	07LT6-1	06LT3-2	06LT3-2	07LT6-1	07LT6-1	07LT6-1
Locality	m	i	sy	m	nc	sy	sy	sy	sy
<b>SiO<sub>2</sub></b>	0.00	0.00	53.28	54.39	54.89	51.22	42.26	58.82	55.19
<b>TiO<sub>2</sub></b>	0.02	0.00	0.18	0.03	0.00	0.08	0.86	0.02	0.04
<b>Al<sub>2</sub>O<sub>3</sub></b>	0.01	0.00	1.33	3.90	2.10	0.36	14.94	25.93	28.5
<b>FeO</b>	0.17	0.37	7.10	6.59	18.9	29.73	13.53	0.36	0.54
<b>Cr<sub>2</sub>O<sub>3</sub></b>	0.01	0.01	0.11	0	0.01	0.01	0.16	0.00	0.00
<b>MnO</b>	0.02	0.00	0.10	0.03	0.13	0.47	0.06	0.02	0.01
<b>MgO</b>	0.08	0.04	14.81	13.99	23.42	17.75	11.15	0.02	0.02
<b>CaO</b>	55.69	54.45	22.61	20.35	0.50	0.59	9.33	6.98	10.15
<b>Na<sub>2</sub>O</b>	0.06	0.00	0.42	1.52	0.01	0.02	4.12	7.42	6.02
<b>K<sub>2</sub>O</b>	0.00	0.01	0.01	0.00	0.02	0.00	0.08	0.01	0.02
<b>P<sub>2</sub>O<sub>5</sub></b>	41.13	41.81							
<b>F</b>	1.00	3.09							
<b>Total</b>	98.19	99.78	99.95	100.86	99.98	100.23	96.49	99.58	100.49
<b>O</b>			6	6	6	6	23	8	8
<b>Si</b>			1.969	1.974	2.018	1.968	6.200	2.635	2.480
<b>Al<sup>IV</sup></b>			0.031	0.026	0.000	0.016	1.800	1.368	1.508
<b>Al<sup>VI</sup></b>			0.027	0.141	0.091	0.000	0.781		
<b>Fe<sup>3+</sup></b>			0.022	0.000	0.000	0.045	0.691	0.000	0.000
<b>Ti</b>			0.005	0.001	0.000	0.002	0.095	0.001	0.001
<b>Fe<sup>2+</sup></b>			0.198	0.098	0.581	0.911	0.968	0.013	0.020
<b>Cr</b>			0.003	0	0.000	0.000	0.019	0.000	0.000
<b>Mg</b>			0.816	0.757	1.284	1.017	2.438	0.001	0.001
<b>Mn</b>			0.003	0.002	0.004	0.015	0.007	0.001	0.000
<b>Ca</b>			0.895	0.791	0.020	0.024	1.466	0.335	0.489
<b>Na</b>			0.030	0.107	0.001	0.001	1.172	0.645	0.524
<b>K</b>			0.000	0	0.001	0.000	0.015	0.001	0.001

Note: m, matrix; ng, oriented needle in garnet; nc, oriented needle in clinopyroxene; i, inclusion; sy, symplectite.